Analysis of cell-derived microvesicles that represent novel players in intercellular communication

1. Basic structural studies on microvesicles

1.1. Specific aim #1. To establish a system in which comparable MV subpopulations derived from different functional subsets can be generated on a large scale for studies specified in Specific aims #2-9.

Starting the OTKA project, we realized that standard protocols were missing for the isolation of different intact populations of cell derived extracellular vesicles.
Thus, using T cell hybridomas, T cell lines (such as CCRF CEM or Jurkat cells) as well as magnetically isolated T cell subsets and murine thymus cells we carried out systematic exeriments to assess the composition and integrity of vesicle populations pelleted at different centrifugation times and forces.

Our results regarding the preanalytical and analytical factors that may influence the isolation and correct assessment of extracellular vesicles are as follows:

- We found that ultracentrifugation either at 100 000g or 200 000g may damage microvesicles (100-800 nm vesicles) but not exosomes (vesicles <100 nm in diameter)
- We found that differential centrifugation is not sufficient to obtain homogenous populations of extracellular vesicles. A subsequent size filtration is instrumental for vesicle subset isolation
- We demonstrated that forced filtration may cause fragmentation of larger size vesicles into smaller ones, and may cause substantial damage to microvesicles. As a result, microvesicles appear as empty, blister like structures with disrupted membranes on electron microphotographs. Such „necrotic" microvesicles may serve as sources of „damage associated molecular patterns" (DAMPs), and may significantly confound functional tests using extracellular vesicles
- We have shown that gravity driven size filtration represents a safe and standard way of vesicle isolation
- We concluded that in all experiments, electron microscopy is required as a quality control step for vesicular integrity
- We found that sucrose gradient ultracentrifugation of vesicles is efficient to remove damaged, empty vesicles as well as both microsomal and protein contaminations from vesicle preparations
- We demonstrated that floatation on sucrose gradient does not separate exosomes from microvesicles

With all the methodological experiences mentioned above, we successfully isolated different vesicle populations secreted by the same cellular source including T cell hybridomas, magnetically separated different T cell subpopulations and thymus cells. Our results have led to the establishment of a system in which comparable MV subpopulations derived from different functional T cell subsets may be isolated simultaneously, and our protocols can be used for production and assessment of vesicle production by both T cell hybridomas and primary, bioreactor-cultured T cells.

Transmission electron microscopy showing the simultaneous presence of different subpopulations of secreted extracellular vesicles (including exosomes < 100 nm in diameter and microvesicles with 100-800 nm diameter) in tissue culture supernatant.

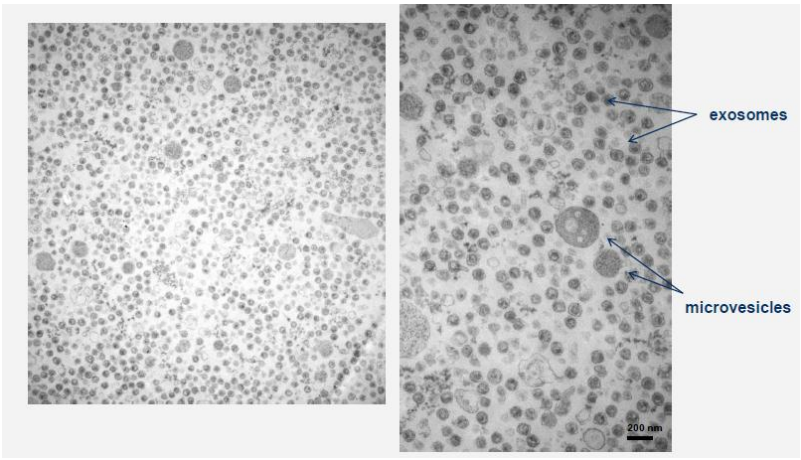

Electron microphotograph of microvesicles isolated by the combination of differential centrifugation and gravity driven size filtration. The intact microvesicles have variable size, are bound by intact membrane of phospholipid bilayer, and their content is fluffy and weakly electron dense.

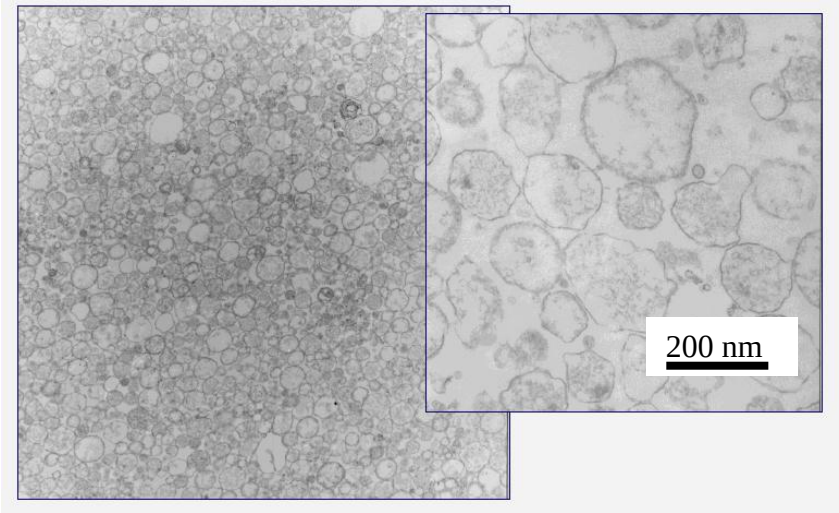

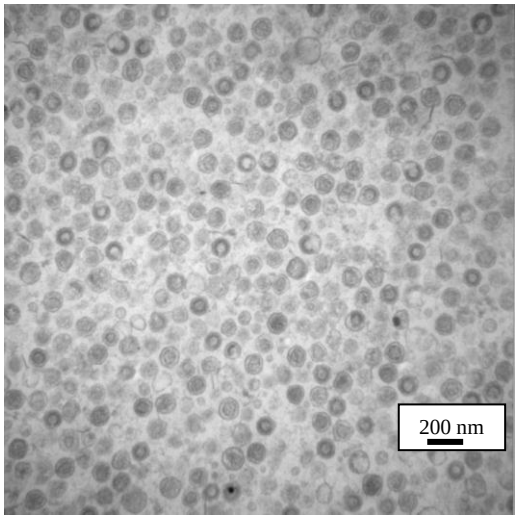

Electron microphotograph of exosomes with typical cup shaped appearence. The 5/4E8 Th1 T cell hybridoma-derived exosomes were isolated by the combination of differential centrifugation, gravity driven size filtration and sucrose gardient ultracentrifugation The exosomes were isolated between densities of 1.13-1.19 g/ml. As compared to electronmicrophotographs routinely taken by other groups in the case of which a drop of vesicle suspension is placed on a grid, we used ultrathin sections of resin embedded vesicular pellets. This way we could analyse substantially higher number of vesicles (exosomes) per electron microscopic field than by the conventional drop analysis method.

1.2. Specific aim #2. To carry out basic characterization of microvesicle subpopulations by using flow cytometric immunophenotyping as well as EM and immune EM techniques in order to control/validate the efficacy of separation techniques or in order to isolate different MV subpopulations (exosomes, ectosomes and apoptotic bodies).

Detection and isolation of cell-derived microparticles are compromised by protein complexes resulting from shared biophysical parameters

Numerous diseases, recently reported to associate with elevated microvesicle/microparticle (MV) counts, have also long been known to be characterized by accelerated immune complex (IC) formation. The goal of our experiments was to investigate the potential overlap between parameters of protein complexes (e.g., ICs or avidin-biotin complexes) and MVs, which might perturb detection and/or isolation of MVs. In this work, after comprehensive characterization of MPs by electron microscopy, atomic force microscopy, dynamic light-scattering analysis, and flow cytometry, for the first time, we drove attention to the fact that protein complexes, especially insoluble ICs, overlap in biophysical properties (size, light scattering, and sedimentation) with MVs. This, in turn, affects MV quantification by flow cytometry and purification by differential centrifugation, especially in diseases in which IC formation is common, including not only autoimmune diseases, but also hematologic disorders, infections, and cancer. These data may necessitate reevaluation of certain published data on patient-derived MVs and contribute to correct the clinical laboratory assessment of the presence and biologic functions of MVs in health and disease.

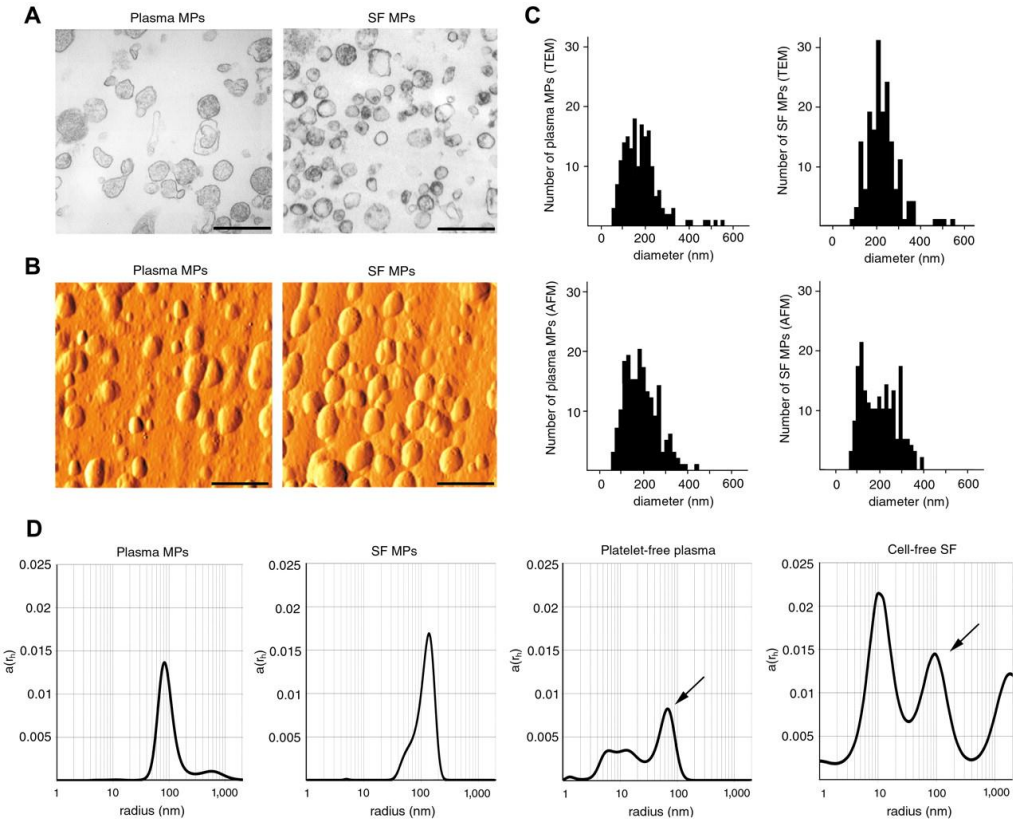

Size distribution analysis of rheumatoid arthritis (RA) plasma and synovial fluid (SF) derived microvesicles by transmission electron microscopy (A), atomic force microscopy (B). C: Size distributions micorvesicles were determined based on TEM and AFM by ImageJ software.
D: Analysis of isolated MVs and native biologic samples by dynamic light scattering (DLS). The x-axis is set to logarithmic scale; a(rh) denotes the coefficient of autocorrelation function of the scattered electric field. Arrows indicate peaks corresponding to MVs in the native samples.

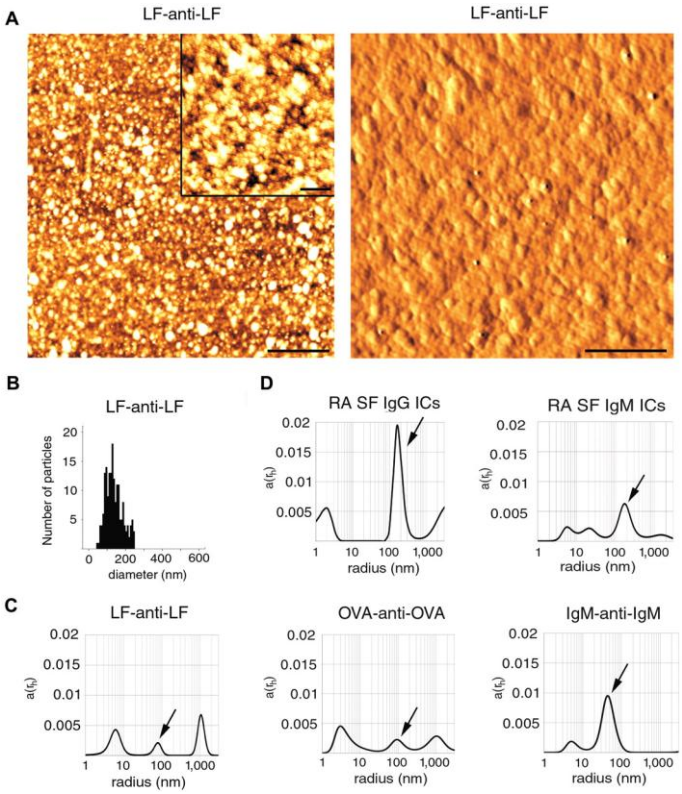

Size determination of immune complexes. (A) AFM images of lactoferrin (LF)-anti-lactoferrin, artificial immune cmplexes. Scale bar represents 1 μm on the left panel. (Inset) Scale bar represents 200 nm. (Right panel) Scale bar represents 250 nm. (B) The histogram represents particle size distribution. For the analysis of particles, ImageJ software (Version 1.42q) was used. (C) Dynamic light scattering (DLS) analysis of LF-anti-LF, OVA-anti-OVA, IgM-anti-IgM ICs. Arrows indicate peaks overlapping with MV sizes. (D) RA SF immune complexes were isolated on an anti-IgG and anti-IgM agarose columns and were also analyzed by DLS. Arrows indicate peaks overlapping with MV sizes. The x-axis is set to logarithmic scale; a(rh) denotes the coefficient of autocorrelation function of the scattered electric field.

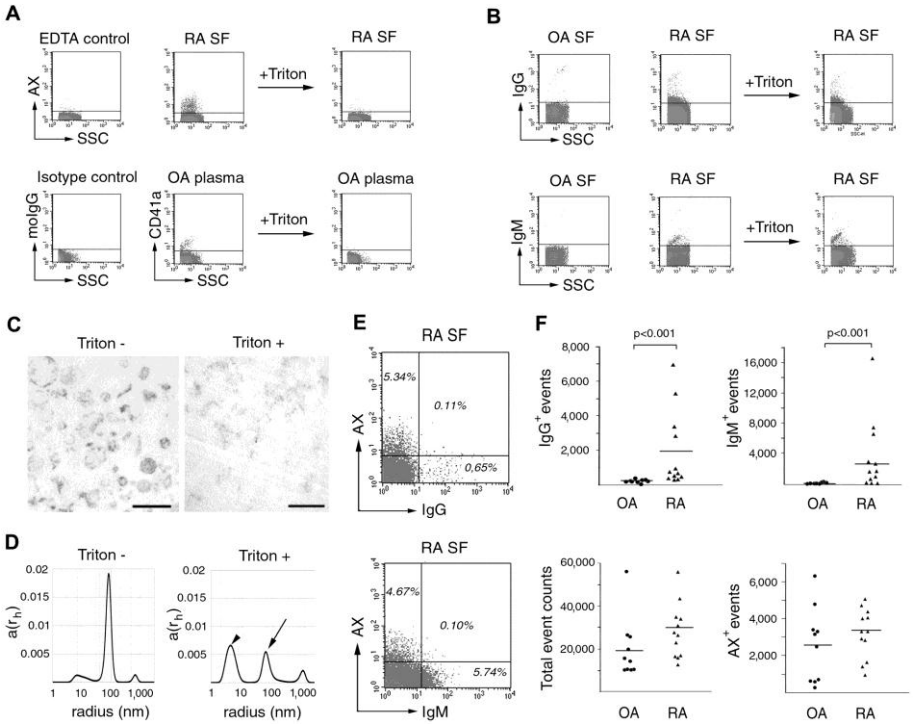

Flow cytometry of microvesicles (MVs) and immune complexes (ICs).

(A) MVs from RA synovial fluid and osteoarthritis (OA) plasma have been stained with AX-FITC or CD41a-FITC and were subjected to detergent lysis by 0.05% Triton X-100. moIgG denotes antimouse IgG used for isotype control. (B) SFs from OA and RA patients were stained with anti-IgG-FITC or anti-IgM-FITC and were also subjected to detergent lysis by 0.05% Triton X-100. All plots represent events from the MV gate. (C) To prove MV lysis, isolated MVs were visualized by TEM before and after lysis. Original magnification × 20 000. Scale bars indicate 400 nm. (D) DLS of MPs before and after addition of detergent. The x-axis is set to logarithmic scale; a(rh) denotes the coefficient of autocorrelation function of the scattered electric field. Arrow indicates the remaining MP-related signal. Arrowhead indicates the signal of Triton X-100. DLS experiments were carried out at 21°C. (E) Dot plots of RA SFs stained with AX-PE and anti-IgG-FITC or anti-IgM-FITC (n = 3 in each group). Events are shown within the R1 gate. (F) IgG+, IgM+, total, and AX+ event counts within the MV of RA and OA SFs. Horizontal lines indicate mean values. The P values were obtained from Mann-Whitney test (n = 21).

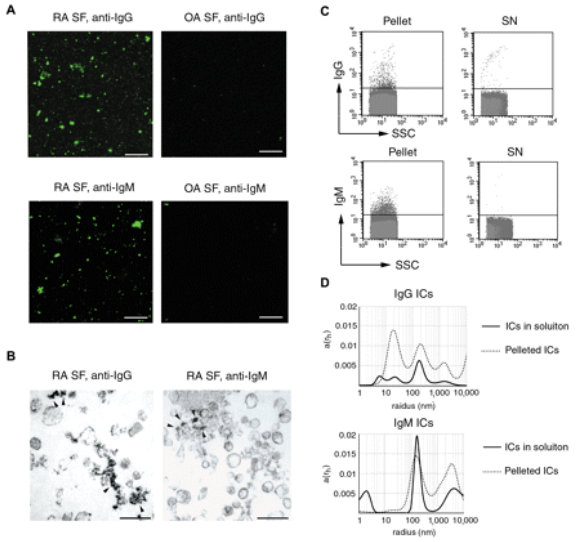

Co-sedimentation of ICs and MVs. (A) Fluorescent microscopy images of anti-human IgG-FITC or anti-human IgM-FITC-stained 20 500g pellets from RA and OA SFs. Images were captured at room temperature using a Zeiss LSM 510 Meta confocal laser scanning microscope equipped with an inverted Axiovert 200M microscope, 63× Plan Apochromat oil immersion differential interference contrast objectives (numerical aperture, 1.4). The acquisition software was AIM LSM, Version 4.2. (B) The 20 500g pellet from RA SF was analyzed by immune EM, stained with antihuman IgG-HRP or antihuman IgM-HRP. Arrowheads indicate immunopositive structures among MPs. Original magnification × 50 000. Scale bar represents 400 nm. Images were captured at room temperature using Hitachi 7100 electron microscope equipped with a Megaview II digital camera. (C) FC analysis revealed that isolated ICs were present in the pellet and were nearly absent in the supernatant (SN).

Our findings do not only imply that immune complexes (ICs) may confound results obtained during microvesicle assessment, but have broader consequences. Indirect immunolabeling, avidin-biotin complexes, and the self-aggregation of an antibody may also lead to MV-mimicking signals, which are detergent resistant. Of importance, the overlapping parameters of ICs and MVs may also affect the purity of isolated MV preparations. Most workgroups apply differential-centrifugation protocols to prepare MVs. In this study, we show that both artificial and natural ICs may contaminate the so-called "MV pellet." Consistent with our findings, a recent report has documented the presence of proteinaceous contamination in urinary microvesicle preparations. Given the well-known ability of ICs to provoke robust biologic responses, functional assays that use MVs isolated by differential centrifugation may lead to misleading results. Therefore, for functional assays of MVs, annexin V or other surface marker-based affinity isolation is highly recommended.
Our findings also have relevance to nonrheumatologic diseases, such as acute coronary syndrome and sickle cell disease in which the presence of circulating ICs is well documented and may cause interference with MV detection.

Our data bring attention to the substantial size overlap between MVs and ICs that may falsify both detection results and functional assays of MVs. Whether these findings also imply that *in vivo* MVs may penetrate and deposit tissue spaces described previously to be accessible for ICs remains to be answered.

(Detection and isolation of cell-derived microparticles are compromised by protein complexes resulting from shared biophysical parameters. György B, Módos K, Pállinger E, Pálóczi K, Pásztói M, Misják P, Deli MA, Sipos A, Szalai A, Voszka I, Polgár A, Tóth K, Csete M, Nagy G, Gay S, Falus A, Kittel A, Buzás EI.
Blood. 2011 Jan 27;117(4):e39-48.)

1.3. Specific aim #3. To investigate the hypothesis that microvesicles can be considered as live objects in any sense for a certain period of time

In order to assess the question of extracellular vesicles may be considered as live objects, first we tested if they contained ATP. Using a Molecular Probes' ATP Determination Kit (A22066) we could not detect the presence of ATP within vesicles possibly due to the low amount of ATP within these structures and the relatively high background noise.
Next we addressed the question as to whether extracellular vesicles were characterized by an autonomous ion homeostasis.

To test if MVs carry Na/K ATP-ase, we stained plasma samples as well as isolated MVs from healthy human plasma with Bodipy FL ouabain (Life Technologies) (1 µg for 20 µl plasma, diluted to 300 µl in Hank's medium). We observed a positive staining within the defined MV gate (not shown).
To determine if this Na/K ATP-ase was functional, we added unlabeled ouabain to isolated MVs from human plasma. For MV isolation, we used platelet-free plasma, MVs were pelleted at 20,500g. After washing in Na/K ATP-ase buffer, MVs were resuspended in 100 µl of 0.9% or 2% NaCl solution. MVs were stained using sodium green (10 µM final concentration, Life Technologies) for 30' at 37 °C. Ouabain was added after diluting the samples to 300 µl for flow cytometry. We observed a time-dependent decrease in the sodium green positive events, indicating that MVs were disrupted allowing the dye to leak out.

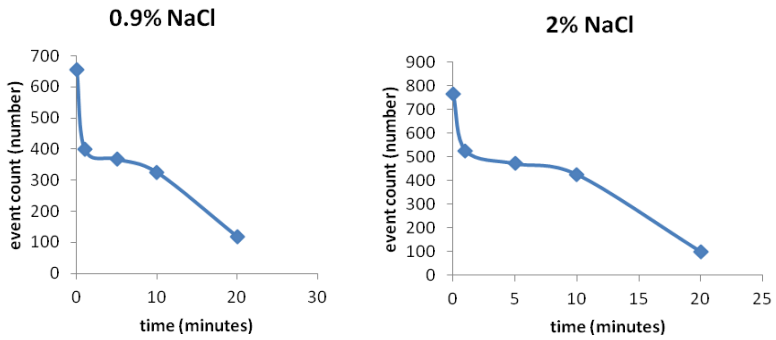

The effect of ouabain on MV numbers.

The effect of A23187 on MVs

To test membrane integrity and to develop a simple method for MV quality control, we hypothesized that the Ca(2+) signal was increased in intact MVs after the addition of an ionophore (A23187). We isolated MVs from human plasma (see above), as well as from cell cultures of CCRF and U937 cell lines using similar centrifugation protocols. MVs were stained with Fluo-4 (10 µM final concentration) for 30 minutes at 37 °C. Before measurement, the dye was washed out and samples were diluted to 300 µl for FACS analysis. A23187 was added to the samples (100 µM final concentration, 10 minutes incubation). We observed an increase in the Ca(2+) concentration in all tested samples, indicating an intact cell membrane.

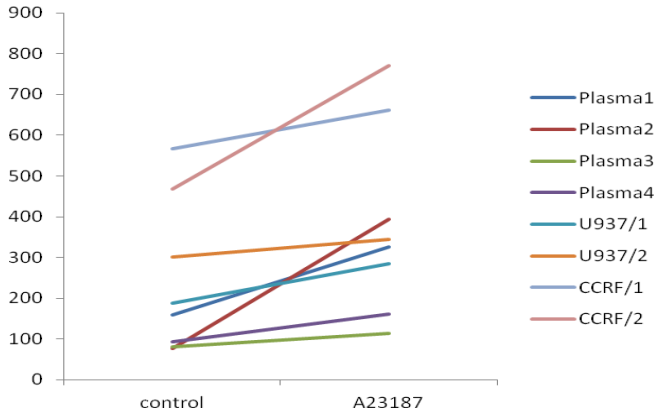

Fig. 2. The effect of A23187 on MV Ca(2+) concentrations. The y axis represents the fluorescent event numbers within the MV gate. (Bence Gyorgy et al. Manuscript in preparation)

1.4. Specific aim #4. To characterize molecular differences among microvesicle populations by using mass spectrometry (MS).

1.4.1.Proteomic characterization of thymocyte-derived microvesicles and apoptotic bodies in BALB/c mice

We set the goal of proteomic characterization of two less studied populations of extracellular vesicles, microvesicles (100-800 nm) and apoptotic bodies (> 800 nm) released by thymus cells of BALB/c mice. The vesicles were isolated by the combination of differential centrifugation and gravity driven multistep filtration of the supernatant of thymus cell cultures. The size distribution of vesicle preparations was determined by transmission electron microscopy. Proteins were released from the vesicles, digested in solution, and analyzed using nano-HPLC/MS(MS). Ingenuity pathway analysis was used to identify functions related to membrane vesicle proteins. In apoptotic bodies and microvesicles we have identified 142 and 195 proteins, respectively. A striking overlap was detected between the proteomic compositions of the two subcellular structures as 108 proteins were detected in both preparations. Identified proteins included autoantigens implicated in human autoimmune diseases, key regulators of T-cell activation, molecules involved in known immune functions or in leukocyte rolling and transendothelial transmigration. The presence and abundance of proteins with high immunological relevance within thymocyte-derived apoptotic bodies and microvesicles raise the possibility that these subcellular structures may substantially modulate T-cell maturation processes within the thymus**.**
(Proteomic characterization of thymocyte-derived microvesicles and apoptotic bodies in BALB/c mice. Turiák L, Misják P, Szabó TG, Aradi B, Pálóczi K, Ozohanics O, Drahos L, Kittel A, Falus A, Buzás EI, Vékey K.J Proteomics. 2011 Sep 6;74(10):2025-33.)

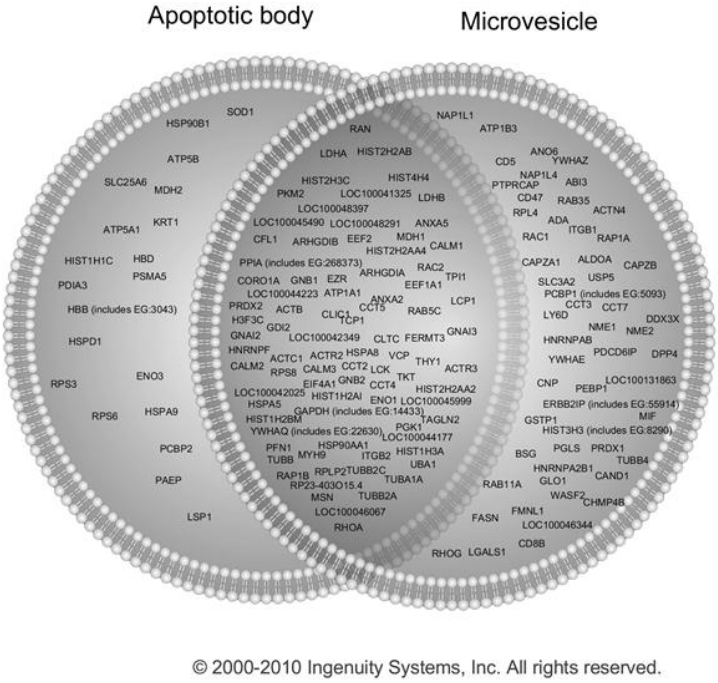

Proteins identified in thymus-derived apoptotic bodies and microvesicles by nano-HPLC/MS(MS).

1.4.2.Mass spectrometry analysis of synovial fluid microvesicles

In this work microvesicles were isolated by differential centrifugation from synovial fluid samples of 3 rheumatoid arthritis (RA), 3 osteoarthritis (OA) and 3 JIA (juvenile idiopathic arthritis) patients. The vesicles were visualized by transmission electron microscopy (TEM), the protein content of microvesicle preparations was determined by a micro-BCA kit, and their composition was analysed by mass spectrometry.

In all microvesicle preparations electron microscopy confirmed the presence vesicles with a diameter of 80- 400 nm. However, among the vesicles, in all preparations significant amounts of amorphous substance was also observed. The protein content of the vesicle preparations of RA samples (0.88 ± 0.63 mg/ml) and of JIA samples (0.51 ± 0.48 mg/ml) were higher as compared to OA samples (0.14 ± 0.10 mg/ml) (not significant). Using mass spectrometry, in RA we identified 98, in OA we found 105, and in JIA we identified 88 proteins. Canonical extracellular vesicle proteins were present in all preparations (including cytoskeletal proteins such as actin, tubulin and myosin, enzymes (pyruvate kinase, triose phosphate isomerase, alpha enolase) as well as

membrane molecules (MHC-I, MCH-II and Na/K ATP-ase). The preparations isolated from the different patient groups showed highly similar protein patterns. In the meantime, besides typical microvesicle proteins, we also identified large amounts of plasma proteins (albumin, transferrin, fibrinogen, prothrombin, haptoglobin.) and immune complex proteins (complement proteins, immunoglobulins). In conclusion, the protein composition of microvesicles isolated from synovial fluid samples of patients with various joint diseases, did not differ significantly. However, our work drives attention to the fact that protein aggregates and immune complexes that fall into the size range of microvesicles, may contaminate microvesicle preparations. Considering the potential use of microvesicles as biomarkers, it is instrumental to consider the possible presence of non-vesicular particles in the preparations.

2. Basic functional studies on microvesicles

2.1. Specific aim #5. Functional characterization of the consequences of the crosstalk of immune cells mediated by MVs

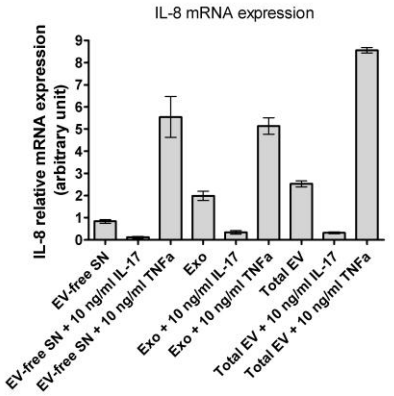

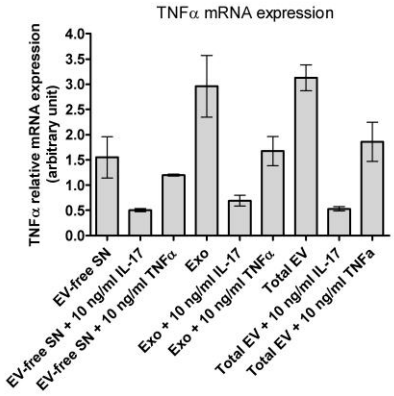

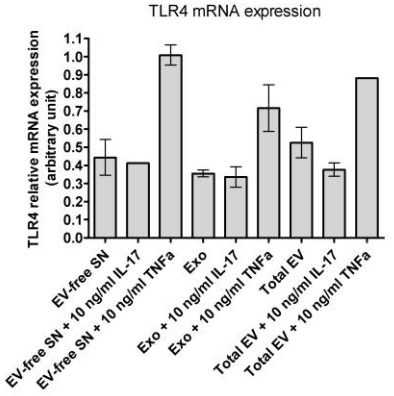

For the first time, we tested if there was a crosstalk between secreted extracellular vesicles and T helper cell subset-specific cytokines (such as TNF or IL-17) on monocytes.
CCRF cells were grown in serum-free RPMI. Extracellular vesicle (EV) production was allowed to take place for 24 hours. Subsequently, the supernatant was used to produce **i)** supernatant (SN) containing a combination of different types of EVs; **ii)** supernatant containing only exosomes (Exo); **iii)** vesicle-free supernatant (EV-free SN)
Monocyte cell line U937 was added to the different supernatants. In order to monitor cross-talk between EVs and cytokines, some of the wells each containing different EV fractions, were treated with 10 ng/ml IL-17 or 10 ng/ml TNFα, respectively. The cells were incubated for 24 hours before total RNA extraction. Quantitative real-time PCR of selected genes including HGPRT as an endogenous control, TNFα, IFNγ, TGFβ receptors 1 and 2, IL-6, IL-10, IL-17a and f, IL-22, IL-23a, TLR 2 and TLR4 was performed using Taqman gen expression assays
Among the analysed genes, the mRNA levels of IL-8, TNFα and TLR4 changed following the treatment with a combination of cytokines and EV from CCRF T-cells.
The expression of IL-8 decreased following treatment with IL-17a, but increased after treatment with TNFα. Remarkably, treatment with exosomes or mixed EVs derived from CCRF cells was sufficient to induce increased expression of IL-8, and a combination of mixed EVs and TNFα was the most efficient inducer of IL-8 expression supporting the idea of a cross-talk between cytokines and EV.
The expression of TNFα was induced by CCRF supernatants containing exosomes and mixed EVs. The cytokine IL-17 appeared to have a negative regulatory effect on TNFα mRNA expression, and EVs from CCRF cells was not sufficient to counteract this effect.
The expression of TLR4 was induced by treatment with TNFα, and this effect was decreased by EV from CCRF cells, again in support of the existence of a cross-talk between EV and cytokines.

Katalin Szabo-Taylor, Krisztina Pálóczy, Tamas Geza Szabo, Borbala Aradi, Andras Falus, Edit I Buzas, manuscript in preparation

Specific aim #6. To compare the miRNA expression of different T cell subsets and their cellular and microvesical miRNA pattern

Naive and nTreg murine CD4+ T cells were isolated from spleens of BALB/c mice by magnetic cell isolation (Miltenyi Biotec GmbH). Magnetically isolated cell populations as well as the 5/4E8 T cell hybridoma and primary thymus cells were used as sources of various extracellular vesicle populations. RNA-extraction was carried out by miRNeasy Mini Kit, Quiagen. The sample quality control was be performed by using Bioanalyzer 2100 (Agilent). Real-time RT-PCR. (human Taqman® miRNA Assays, Applied Biosystem) was used to identify certain miRNAs.

The RNA profiles of cells significantly differed both from that of microvesicles and exosomes. Strikingly, exosomes were characterized by the absence of the 18S and 28S ribosomal RNA peaks, and contained large amounts of small RNA molecules.

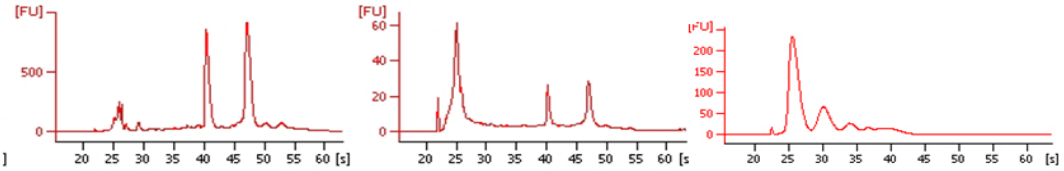

cell	microvesicles	exosomes
n=3	n=3	n=7
miRNA/total RNA%		
31%	**30%**	**51,29**
SD=8.72	SD=9.17	SD=4.11

In the cells and cell-derived extracellular vesicles we showed the presence of sno142, **miR155, mir146 and miR150, miR21 and miR123.**

Clearly, exosomes were found to be enriched in miRNAs as compared to microvesicles.

3. Studies on the *in vivo* function of microvesicles

3.1. Specific aim #7. To assess pathogenic/arthritogenic features of microvesicles

Groups of adult female BALB/c mice (n=6 in each group) were injected either with washed, mixed EVs isolated by ultracentrifugation from normal mouse blood plasma, resuspended in PBS or PBS alone, intraarticularly (to the ipsi- and contralateral knee joints, respectively). The mice were observed daily after the injection, for periarticular swelling or redness. Mice were sacrificed after 3 weeks, the knee joints were fixed, decalcified and Haematoxylin and Eosin stained sections were analyzed by light microscopy.

No sign of inflammation was observed in any of the injected joints (not shown).

3.2. Specific aim #8. To investigate the correlation of serum/plasma microvesicular composition with disease activity

We investigated the role of microvesicles in polymyositis/dermatomyositis, a group of rare autoimmune diseases, characterized by specific skin lesions and muscle weakness. The plasma concentration of monocyte and lymphocyte derived microvesicles of 20 patients with polymyositis/dermatomyositis and 20 healthy controls were determined by flow cytometry. The structure of microvesicles was visualized by electron microscopy. Significantly elevated numbers of monocyte (CD14 positive), T-lymphocyte (CD3 positive) and B-lymphocyte (CD19 positive) derived microvesicles were found in the plasma samples of polymyositis/dermatomyositis patients, compared to healthy controls ($p = 0.001$, 0.01 and 0.006, respectively).

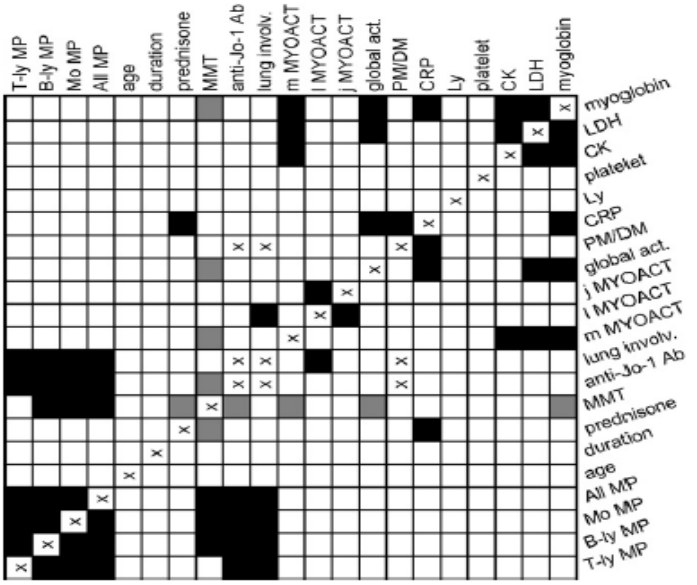

Fig. 3. Correlation matrix of MP counts, clinical and laboratory parameters. Significant positive and negative correlations are marked by black and gray colors, respectively. Non-significant and non-calculated correlations are marked by white color and letter X, respectively. Parameters of the matrix (sometimes abbreviated): T-ly MP – T-lymphocyte derived MPs; B-ly MP – B-lymphocyte MPs; Mo MPs – Monocyte derived MPs; All MPs; duration – duration of illness; prednisone – dose of prednisone; MMT; anti-Jo-1 Ab – anti-Jo-1 antibody; lung involv. – lung involvement; m MYOACT – MYOACT for muscle; l MYOACT – MYOACT for lung; j MYOACT – MYOACT for joint; global act. – global activity; PM/DM – diagnosis of PM/DM; CRP; Ly – lymphocyte; platelet; CK; LDH; myoglobin. $n = 20$; $p = 0.05$.

Furthermore, the plasma levels of monocyte and B-lymphocyte derived microvesicles correlated with the manual muscle strength test (r = 0.497, p = 0.027; r = 0.508, p = 0.023; respectively). Patients with anti-Jo-1 antibody and lung involvement had significantly higher numbers of T- and B-lymphocyte and monocyte derived MPs (p = 0.006, 0.012 and 0.007, respectively, for anti-Jo-1; p = 0.013, 0.016 and 0.025, respectively, for lung involvement). After ultracentrifugation, CK activity could be detected only in traces in the resuspended pellet containing microparticles of healthy and diseased individuals. The electron microscopy revealed slightly different microvesicles in the samples of patients with polymyositis/dermatomyositis. These results suggest that immune cell derived microvesicles may contribute to the inflammatory process in polymyositis/dermatomyositis, however, CK-positive, possibly muscle derived microsicles do not seem to be present in the blood of patients with polymyositis/dermatomyositis. ***(Increased serum concentration of immune cell derived microparticles in polymyositis/dermatomyositis. Baka Z, Senolt L, Vencovsky J, Mann H, Simon PS, Kittel A, Buzás E, Nagy G. Immunol Lett. 2010 Feb 16;128(2):124-30***

3.3. Specific aim #9. To investigate the immunoregulatory role of microvesicles in foetomaternal communication

We described for the first time the *in vivo* plasma pattern of microvesicles of the third-trimester healthy pregnant women, their cellular origin and their target cells using flow cytometry and confocal microscopy. Neutralizing antibodies were used to identify cellular targets of molecules of platelet derived microvesicles. We studied the *in vitro* effects of microvesicles on STAT3 phosphorylation testing primary lymphocytes and Jurkat T cells. We found that that both placental trophoblast-derived and maternal platelet-derived microvesicles bind to circulating peripheral T lymphocytes, but not to B cells or NK cells. We showed that the P-selectin (CD62P)-PSGL1(CD161) interaction was involved in binding of platelet –derived microvesicles to T cells. We provided evidence that microvesicle-T cell interactions induce STAT3 phosphorylation in T lymphocytes. These data indicate that both platelet- and trophoblast-derived microvesicles may play a role in the immunoregulation of pregnancy. Our findings suggest that the transfer of different signals via microvesicles represents a novel form of communication between the placenta and the maternal immune system, and that microvesicles contribute to the establishment of stable immune tolerance to the semi-allograft fetus (***Pap E, Pállinger E, Falus A, Kiss AA, Kittel A, Kovács P, Buzás EI. T lymphocytes are targets for platelet- and trophoblast-derived microvesicles during pregnancy.***

Placenta. 2008 Sep;29(9):826-32.).

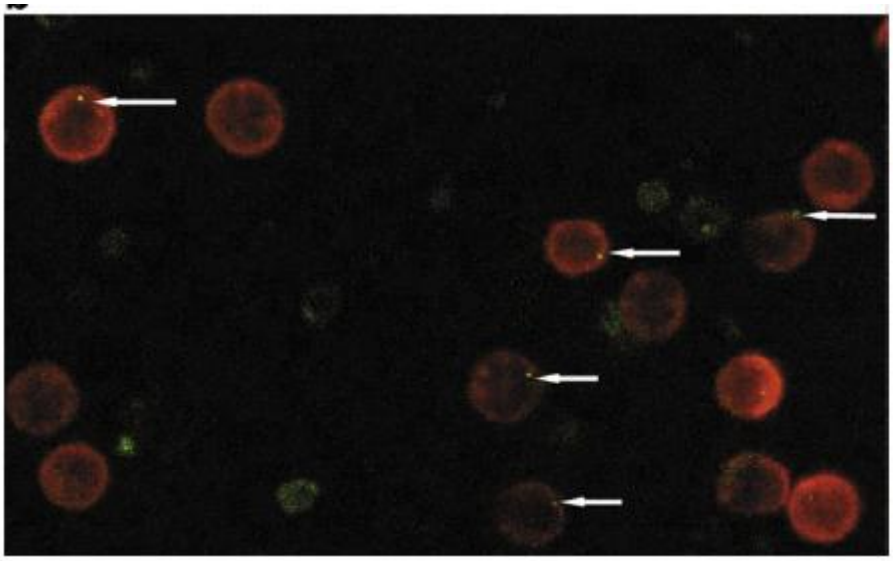

Trophoblast-derived (HLA G+) microvesicles bind to T cells. Healthy woman donor-derived peripheral T cells are labelled with a PE-conjugated anti-CD2, anti-CD3, anti-CD5 and anti-CD7 antibody coctail. Microvesicles isolated from healthy pregnant blood plasma were stained with FITC-conjugated anti-HLAG antibody, and were incubated with the T cells for 30' at 37 ^{o}C. The green extracellular vesicles are seen on the surface of th ered labelled T cells.

On the following figure panel „a" shows binding of CD41a+ platelet-derived microvesicles to T cells. The „b" panel shows the binding of microvesicles following a preincubation with an anti- CD62P monoclonal antibody, while panel „c" demonstrates the microvesicle binding to T cells after preincubation T lymphocytes with an anti-CD162 antibody.